Translational Oncology 31 (2023) 101644

Contents lists available at ScienceDirect

Translational Oncology

journal homepage: www.elsevier.com/locate/tranon

Original Research

CD44 occurring alternative splicing promotes cisplatin resistance and evokes tumor immune response in oral squamous cell carcinoma cells

Xue Qiao [a,b], Li Zhu [a], Rongbo Song [a], Chao Shang [c], Yan Guo [a,b,*]

[a] Department of Central Laboratory, School and Hospital of Stomatology, Liaoning Provincial Key Laboratory of Oral Disease, China Medical University, Shenyang, Liaoning 110002, China
[b] Department of Oral Biology, School and Hospital of Stomatology, Liaoning Provincial Key Laboratory of Oral Disease, China Medical University, Shenyang, Liaoning, China
[c] Department of Neurobiology, China Medical University, Shenyang, Liaoning, China

ARTICLE INFO

Keywords:
Alternative splicing
CD44
Cisplatin resistance
Dendritic cells
Tumor immune response
Oral squamous cell carcinoma

ABSTRACT

Background: Oral squamous cell carcinoma (OSCC) is the most prevalent malignant tumor in head and neck region. Platinum drug resistance limits the clinical application of chemotherapy regardless of medical development. The aim of our study is to identify cisplatin-resistant genes which can be used as new therapeutic targets and investigate the functional mechanism of OSCC chemoresistance.

Methods: The OSCC Cal27 and HSC4 cisplatin-resistant cell lines were constructed to screen the differential genes/transcripts expression. GO, KEGG and GSEA were performed to reveal the relevant signaling pathways. Alternative splicing (AS) software rMATs was applied to explore AS events in chemoresistance. R package and TIMER tools were used to evaluate the linear correlation between CD44 and immune cell subpopulations. The co-culture model of dendritic cells (DCs) and OSCC cells was applied to explore the effect of CD44 on immune microenvironment and cisplatin resistance.

Results: Our results showed that CD44 was differentially expressed in cisplatin-resistant OSCC cells. Through bioinformatics prediction and experimental verification, we confirmed that CD44 occurring AS was involved in tumor progression and cisplatin resistance. Moreover, CD44 could further enhance the cisplatin resistance of OSCC by activating DCs, making CD44 to be a potential intervention target. We also identified DC as a new target for platinum drugs to stimulate the growth of OSCC.

Conclusion: Our findings not only make it possible to explore new therapeutic methods, such as CD44 inhibitors or antisense oligonucleotides, but also provide insights into the new mechanisms of cisplatin resistance to chemotherapy.

Introduction

Oral squamous cell carcinoma (OSCC) is the most common (approximately 90%) and highly recurrent malignant epithelial tumor in the oral cavity [1]. The treatment of OSCC still depends on surgical resection combined with radiotherapy and chemotherapy. Due to tumor recurrence and drug resistance, the 5-year survival rate remains no significant increase [2]. Platinum drugs are anti-tumor drugs with high activity for a variety of cancers in clinical application, and are also first-line chemotherapy drugs for OSCC. However, the serious toxic and side effects, especially the emergence of chemotherapy resistance, greatly limit the clinical application of platinum chemotherapy drugs [3, 4]. Therefore, it is of great significance to elucidate the mechanism of OSCC platinum resistance.

There are several major opinions concerning drug resistance. First of all, chemotherapy can not only locate and kill tumor cells, but also stimulate immune cells to release chemicals and promote tumor cells growth, leading to treatment tolerance. The second is the redox reaction

Abbreviations: A3SS, alternative 3′ splice sites; A5SS, alternative 5′ splice site; AS, alternative splicing; DCs, dendritic cells; GDSC, genomics of drug sensitivity in cancer; GO, gene ontology; GSEA, gene set enrichment analysis; IR, intron retention; KEGG, kyoto encyclopedia of genes and genomes; MXE, mutually exclusive exon; OSCC, oral squamous cell carcinoma; SE, skipped exon; TCGA, the cancer genome atlas.

* Corresponding author at: Department of Central Laboratory, School and Hospital of Stomatology, Liaoning Provincial Key Laboratory of Oral Disease, China Medical University, Shenyang, Liaoning 110002, China.
E-mail address: yguo@cmu.edu.cn (Y. Guo).

https://doi.org/10.1016/j.tranon.2023.101644
Received 30 November 2022; Received in revised form 9 January 2023; Accepted 15 February 2023

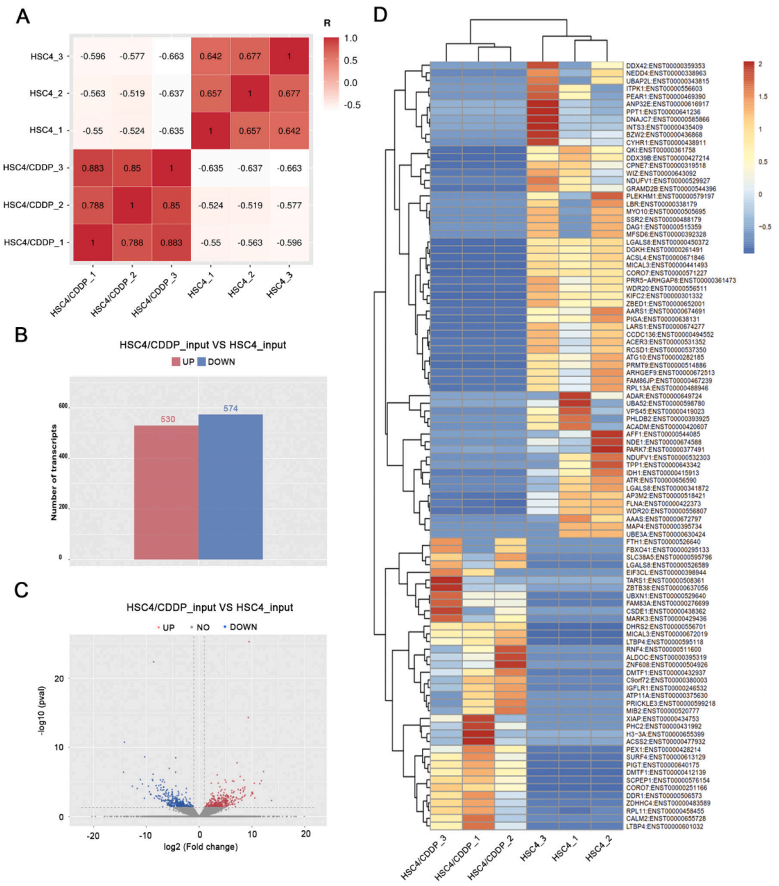

Fig. 1. Differentially expressed mRNAs screened in HSC4/CDDP cells. (A) Sample correlation matrix: the Spearman correlation (R2) was calculated and visualized by color (red-white) in the matrix. (B) The number of both up and down regulated genes in HSC4/CDDP cells relative to HSC4 cells. (C-D) Volcano and heat maps of differentially expressed mRNAs in HSC4 and HSC4/CDDP cells.

of cancer cells, which is the most important factor for the existence and persistence of drug resistance [5]. The third is the generation of new mutations caused by transcription reprogramming after chemotherapy [6,7]. As the first-line treatment and standard care of OSCC, cisplatin (CDDP) mainly produces drug resistance by enhancing DNA repair ability, reducing drug uptake/accumulation, and improving the body tolerance to platinum-DNA complex [8]. Exploring the generation of substances that stimulate the growth of tumor cells in cisplatin resistance has aroused widespread interest. Previous studies showed that tumor microenvironment could more accurately affect the effect of chemotherapy, that is, the same tumor cells in different microenvironments might react differently to the same chemotherapy drugs [9]. *Balkwill F.R.* et al. reported that the chemotherapy process could trigger normal immune cells to attack nearby tumors, and the normal cells near tumors could also promote tumor resistance to chemotherapy [10]. Alternative splicing (AS), as a committed step of post-transcriptional gene regulation, can lead to abnormal expression of downstream target genes and disorder of tumor microenvironment, which is closely related to the occurrence of chemotherapy resistance [11].

In this study, we constructed OSCC Cal27 and HSC4 cisplatin-resistant cell lines to screen the differential genes/transcripts expression and reveal the AS relevant chemotherapy resistance signaling pathways. Through the combination of bioinformatics prediction and experimental verification, we detected the role of CD44 with differential expression and AS in the immune microenvironment, and explored the possible mechanism of cisplatin resistance. The results showed that CD44 could further enhance the cisplatin resistance of OSCC by activating DCs, making CD44 to be a potential intervention target. We also identified DC as a new target for platinum drugs to stimulate the growth of OSCC. Our findings not only make it possible to explore new therapeutic methods, such as CD44 inhibitors or antisense oligonucleotides, but also provides insights into the new mechanisms of cisplatin resistance to chemotherapy.

Materials and methods

Cell lines and culture

We obtained the OSCC cell lines (HSC4, Cal27) and the mouse dendritic cell line (DC2.4) from the Chinese Academy of Sciences in Shanghai. After STR phenotype identification, these cells were cultured at 37°C in a moist atmosphere consisting of 5% CO_2 plus 95% air. The medium was DMEM (Hyclone, USA) with 10% fetal bovine serum (Gibco, USA) supplement. The cisplatin resistant OSCC cells (HSC4/CDDP, Cal27/CDDP) were established as previously described by culturing HSC4 and Cal27 cells with gradually increasing concentration of CDDP (Sigma, USA). In general, a continuing 0.5 μ M CDDP was used to maintain the cells resistance and was removed 7 days before experiments.

Apoptosis analysis

The apoptotic rates of HSC4/CDDP and Cal27/CDDP cells were analyzed using Annexin V-FITC apoptosis detection kit (Biosea, China). Briefly, 2×10^5 cells were collected and centrifuged for 5 min at 1000 rpm and washed at least twice by frozen PBS. Then, cells were resuspended in 300-500 μl binding buffer followed by incubating with 5μl Annexin V-FITC and 5 μl PI staining, respectively. Finally, cells were

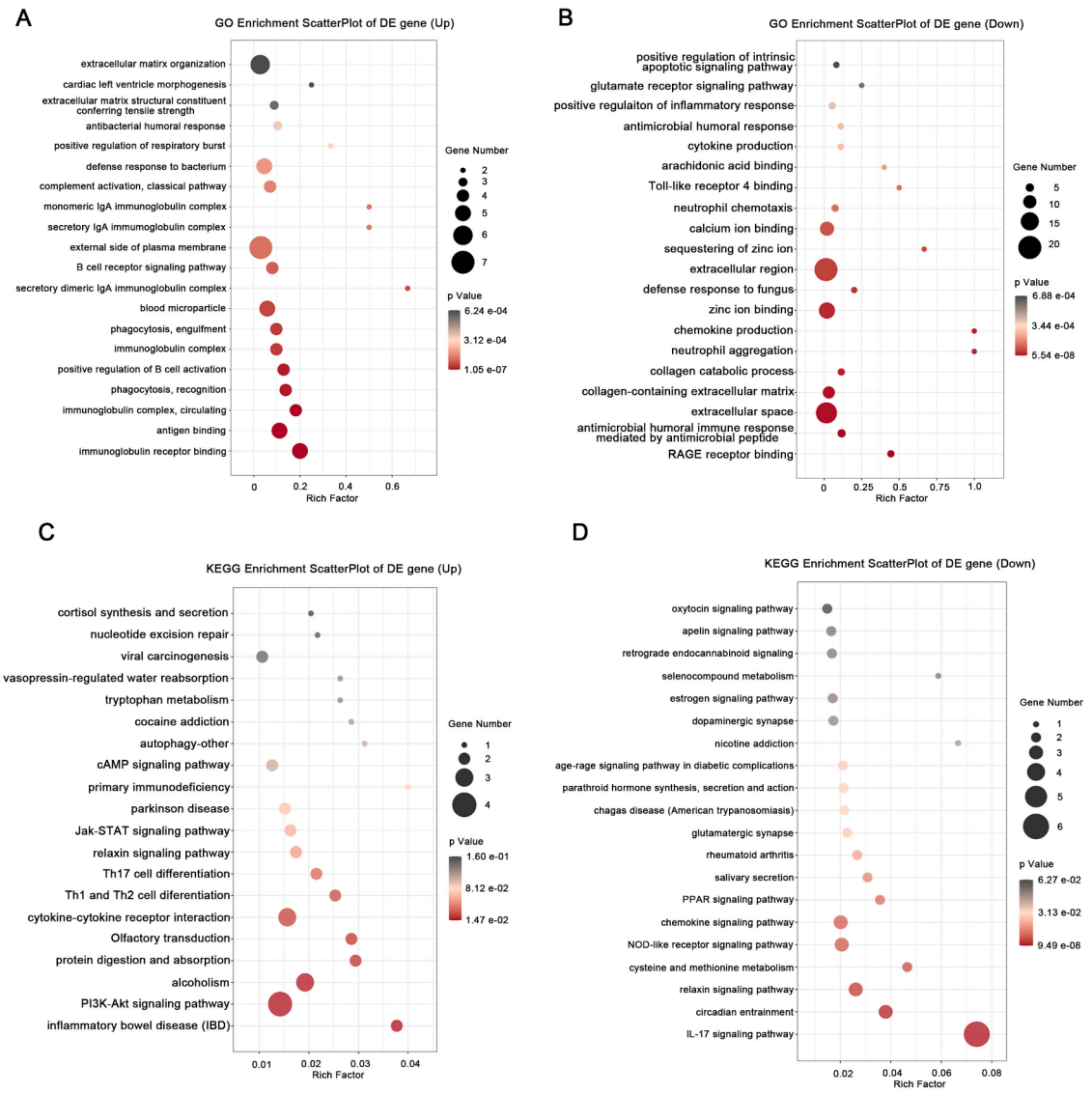

Fig. 2. GO and KEGG pathway analysis in HSC4/CDDP cells. (A, B) Gene ontology (GO) analysis of dysregulated genes in HSC4/CDDP cells compared with HSC4 cells. (C, D) KEGG analysis of differentially expressed genes in HSC4/CDDP cells compared with HSC4 cells.

detected using a CantoII flow cytometry (BD, USA) with Diva 8.0 (BD, USA) software within 1 h.

Identification of differently expressed transcripts and genes

HSC4/CDDP and parental control cells were harvested and total RNA was extracted by Trizol Reagent (Invitrogen, USA). Differential mRNAs expression were screened and recognized with StringTie software and R package edgeR. The differential expression genes were usually evaluated and filtered according to the difference multiples and significance levels. Here, we took the difference multiples FC $>=2$ or FC $<=0.5$ and P value $<=0.05$ as standard and considered genes as differential expression transcripts, and displayed them as significant different expression.

GO (gene ontology) and KEGG (Kyoto encyclopedia of genes and genomes) analysis

Differentially expressed mRNAs were selected and performed GO and KEGG pathway analysis. For GO analysis, the corresponding genes were classified as biological process, cellular component and molecular function. For KEGG analysis, the enriched pathways were demonstrated according to enrichment scores.

AS detection

Software rMATs v4.0.2 was used to screen the differential AS events including alternative 3′ splice sites (A3SS), alternative 5′ splice site (A5SS), mutually exclusive exon (MXE), intron retention (IR) and skipped exon (SE) in HSC4/CDDP cells [12,13]. The threshold was set as $|\Delta$ Percent spliced in (PSI)$| > 0.05$ and false discovery rate (FDR) < 0.1.

Gene set enrichment analysis (GSEA)

GSEA was applied to determine the significance of predefined genes between two biological states. The HNSCC samples were grouped according to CD44 high-/low- expression. Biological processes enriched by CD44 were obtained by GSEA analyses of the cancer genome atlas (TCGA) HNSCC datasets. The parameters were set following $P < 0.05$ and FDR < 0.25.

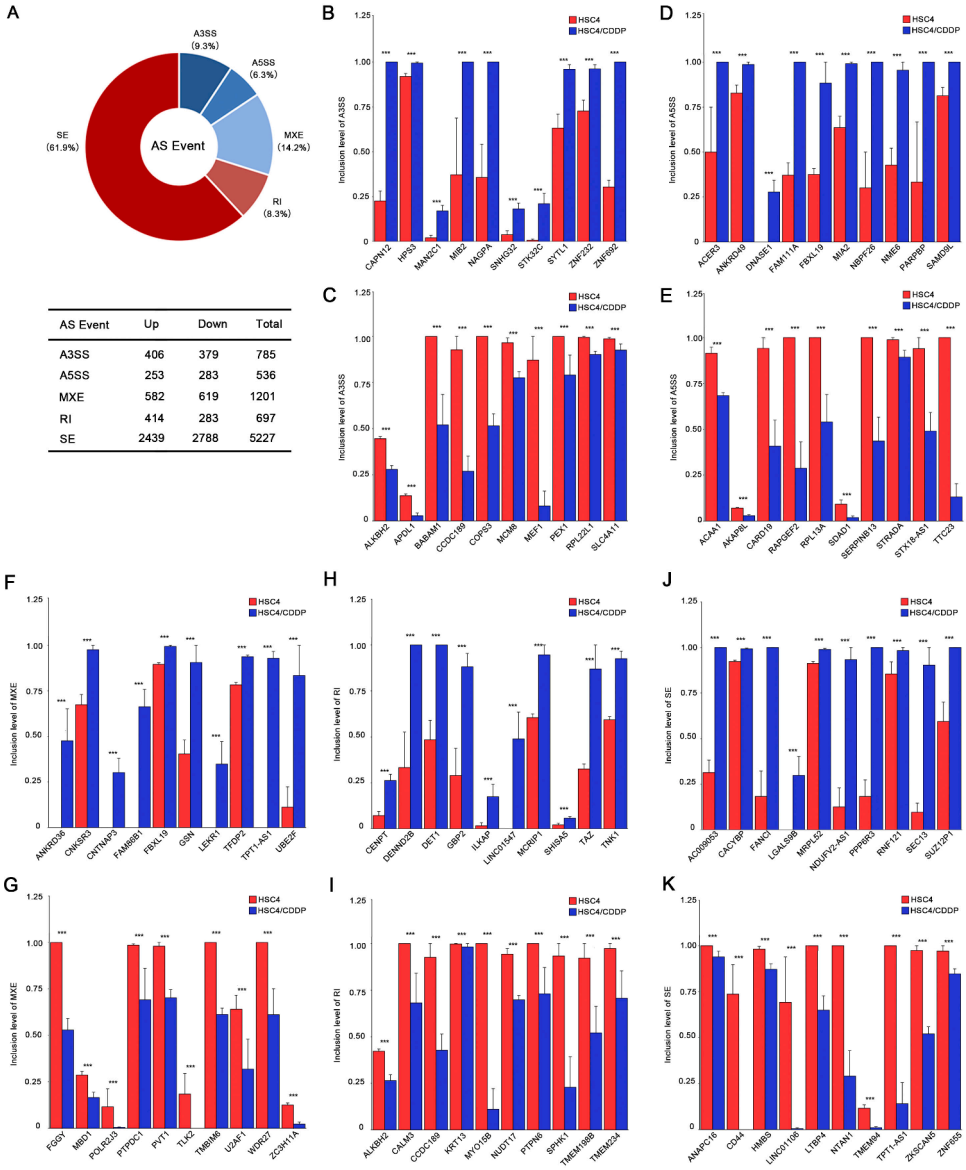

AS Event	Up	Down	Total
A3SS	406	379	785
A5SS	253	283	536
MXE	582	619	1201
RI	414	283	697
SE	2439	2788	5227

Fig. 3. Characteristics of AS events. (A) Pie chart of the percentages of alternative splicing events detected in HSC4 and HSC4/CDDP cells. (B–K) The differential inclusion level of the top 10 upregulated and downregulated genes in A3SS (B, C), A5SS (D, E), MXE (F, G), RI (H, I), and SE (J, K). All experiments were performed at least 3 times; data were shown as mean ± SD. $^{*}P < 0.05$, $^{**}P < 0.01$, $^{***}P < 0.001$ vs. control, Student's *t*-test.

Table 1
Alternative splicing and gene transcription double regulated genes.

Gene Name	AS type	AS expression	Transcription expression	KEGG enrichment pathway	Tumor involved
FANCI	SE	UP ↑	Down ↓	Fanconi anemia pathway	Lung adenocarcinoma Ovarian cancer Breast cancer
ANAPC16	SE	Down ↓	Up ↑	NA	
CD44	SE	Down ↓	Up ↑	ECM-receptor interaction; Hematopoietic cell lineage; Shigellosis; Epstein-Barr virus infection; Proteoglycans in cancer; MicroRNAs in cancer	Breast cancer Colon cancer Prostate cancer Oral cancer Gastrointestinal cancer Renal cancer
LTBP4	SE	Down ↓	Up ↑	NA	Colorectal cancer Hepatocellular carcinoma
MIB2	A3SS	Up ↑	Up ↑	NA	Lung cancer
SYTL1	A3SS	Up ↑	Down ↓	NA	Bladder cancer
RPL22L1	A3SS	Down ↓	Up ↑	Ribosome	Colorectal cancer Ovarian cancer Prostate cancer
PEX1	A3SS	Down ↓	Up ↑	Peroxisome	Lung carcinoma
DENND2B	RI	Up ↑	Down ↓	NA	
TAZ	RI	Up ↑	Down ↓	Glycerophospholipid metabolism	Ovarian cancer Liver cancer Breast cancer Esophageal squamous cell carcinoma Oral squamous cell carcinoma
GSN	MXE	Up ↑	Down ↓	Fc gamma R mediated phagocytosis; Regulation of actin cytoskeleton; Viral carcinogenesis	Bladder cancer Head and neck squamous cell carcinoma Hepatocellular carcinoma Acute myeloid leukemia
CNTNAP3	MXE	Up ↑	Down ↓	NA	Esophageal squamous cell cancer
TLK2	MXE	Down ↓	Up ↑	NA	
ACER3	A5SS	Up ↑	Down ↓	Sphingolipid metabolism	Acute myeloid leukemia Hepatocellular carcinoma
FAM111A	A5SS	Up ↑	Down ↓	NA	
MIA2	A5SS	Up ↑	Down ↓	NA	Oral cancer Other squamous cell carcinoma
SAMD9L	A5SS	Up ↑	Down ↓	NA	Myeloid malignancies
RPL13A	A5SS	Down ↓	Down ↓	Ribosome	Breast cancer Glioblastoma

Immune cell infiltration assessment

HNSCC data were downloaded from TCGA database and sorted into CD44 high-/low- expression groups. Then, CIBERSORT algorithm from the R package was used to obtain immune infiltration chart. TIMER online tool was used to evaluate the linear correlations between CD44 and subpopulations of immune cells.

Plasmid construction and transfection

Genescript (Nanjing, China) constructed CD44 overexpression plasmid (pc-CD44) with the full-length of CD44 cloning into pc-DNA empty plasmid (pc-NC). Then, cells were transfected with Lipofectamine™ 3000 (Invitrogen, USA) following the manufacture instructions after seeding into 6-well plate for 24 h. Western blot were used to confirm the transfection efficiency in this study.

Western blot

Cells were harvested and proteins were purified through RIPA lysis buffer (Beyotime Biotechnology, China). Totally 50μg protein was separated using SDS-PAGE gel. After electrophoresis under 80-120V, the protein was transferred into PVDF membranes. Then the membranes, blocked with 5% skimmed milk for 1 h, were incubated with primary antibodies overnight at 4°C (CD44, Abclonal, 1:1000; GAPDH, Affnity, 1:2000) and secondary antibodies (Abbkine, 1:5000) for 1 h at room temperature. Finally, the bands were obtained using Odyssey Dual Color Infra-Red Laser Imaging System (LI-COR Biosciences, USA) and quantified by Image J software (NIH, USA).

Dendritic cell markers detection

A co-culture model was established with Cal27/HSC4 cells transfected with plasmids seeding into the upper chamber and DC 2.4 cells seeding into the lower chamber of 0.4 μm 6-well transwell plates (Biosharp, China). After co-culturing for 72 h, the DC2.4 cells were resuspended in a 100 μl binding buffer. Then the cells were incubated with 2% anti-CD80, CD86 and MHCII antibodies (BioLegend, USA) for 30 min respectively and then were tested under CantoII flow cytometer (BD, USA) to detect the expression of the markers. Data were calculated and analyzed using FlowJo software (BD, USA).

Statistical analysis

Data were showed as mean ± standard error of measurement and analyzed under two-tailed Student's *t*-test in Prism 5.0 (GraphPad Software, USA). All the experiments were repeated at least triple and $P < 0.05$ was recognized to be of statistical significance.

Results

Establishment of CDDP-resistant OSCC Cell Lines

HSC4 and Cal27 CDDP-resistant cells (HSC4/CDDP and Cal27/CDDP) have been established and stored in our laboratory. Here, to maintain their chemoresistance phenotype, we resuscitated and cultured them in DMEM with 0.5 μM CDDP. Cisplatin resistance was observed in both HSC4/CDDP and Cal27/CDDP cells when compared with parental control cells (Fig. S1A,B). Flow cytometry showed that the

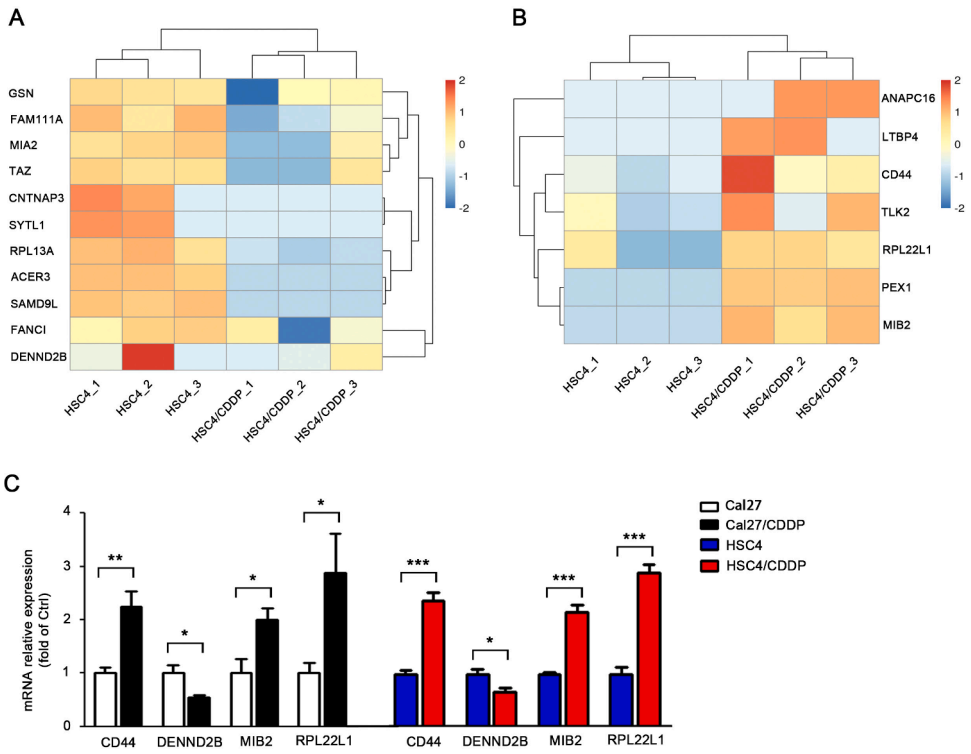

Fig. 4. Differentially expressed mRNAs with AS events in HSC4/CDDP cells compared with HSC4 cells. (A, B) Heat maps of differentially expressed mRNAs with AS events in HSC4 and HSC4/CDDP cells. (C) qRT-PCR used to verify the significant transcriptomic data with AS events. All experiments were performed at least 3 times; data were shown as mean ± SD. *$P < 0.05$, **$P < 0.01$, ***$P < 0.001$ vs. control, Student's *t*-test.

survival rate of HSC4/CDDP and Cal27/CDDP cells was much higher than that of HSC4 and Cal27 cells under a 7.5μM CDDP treatment (Fig. S1C,D).

Analysis of gene/transcript differences in chemoresistance cells

HSC4 and HSC4/CDDP cells were harvested to perform RNA sequencing. Samples correlation analysis showed that the correlation within the replicates for the single group was higher than that between the sample groups (Fig. 1A). The sequencing outcome showed that there were 1104 gene transcripts differentially expressed with the standard of FC >= 2 or FC <= 0.5 (|log FC| >=1) and *P* value <= 0.05, among which there were 530 genes up-regulated and 574 genes down-regulated in HSC4/CDDP cells relative to HSC4 cells (Fig. 1B). Volcano and heat maps were drawn to present the mRNAs expression pattern between the samples (Fig. 1C,D).

GO and KEGG pathway analysis

In order to investigate the potential role of differentially expressed mRNAs in cisplatin chemoresistance, we performed GO enrichment and R package ggplot2 analysis based on the up/down mRNAs expression levels. The results showed that the aberrantly expressed genes were largely enriched for GO terms associated with the regulation of chemokine production, neutrophil arrogation in DE down group, while enriched for GO terms associated with the regulation of immunoglobulin complex, antigen binding and immunoglobulin receptor binding in DE up group. The top 20 most significant GO terms were shown in Fig. 2A and 2B. Moreover, we performed pathway analysis in accordance with the KEGG database, which screened out 20 pathways with most significant differences ($P < 0.05$) in gene expression and were illustrated in Fig. 2C and 2D. These results showed that the downregulated mRNAs were mainly distributed in IL-17 signaling pathway, while the upregulated mRNAs were mainly participated in Th17 cell differentiation, Th1 and Th2 cell differentiation and PI3K-Akt signaling pathway. All these pathways might be associated with OSCC chemoresistance and tumor immune response.

AS Model of HSC4/CDDP cells

A3SS, A5SS, MXE, RI, and SE events were analyzed to clarify the AS potentials in HSC4/CDDP cells (Fig. S2). Totally, there were 6310 AS events, of which 2524 were upregulated and 3786 were downregulated, recognized as differentially expressed in HSC4/CDDP cells relative to HSC4 control cells (Fig. 3A). The percentage of five AS types were 9.3% (A3SS), 6.3% (A5SS), 14.2% (MXE), 8.3% (RI) and 61.9% (SE), respectively. Apparently, SE was the most common AS event in HSC4/CDDP cells. The results revealed that AS events were abundant and intricate in chemoresistance. In order to determine the characteristics of the dysregulated AS events in CDDP resistance, we used rMATs software to validate the top 10 upregulated and downregulated AS events (Fig. 3B–K). The results indicated that AS tended to be a significant molecular event and played a pivotal role in OSCC chemoresistance.

Differentially expressed genes with AS

To elucidate the differentially expressed mRNAs with AS events were closely associated with chemoresistance in HSC4/CDDP cells, we analyzed the top 10 upregulated and downregulated AS events of five classifications according to their different mRNA expression levels. The results showed that among all the 18 correlated genes listed in Table 1, *ANAPC16, LTBP4, CD44, TLK2, RPL22L1, PEX1 and MIB2* occurring AS were upregulated in HSC4/CDDP cells whereas other genes were downregulated (Fig. 4A and 4B). To verify the significance of transcriptomic data with AS, we used qRT-PCR to validate their expression levels. The primers used in the study were listed in Table 2. The results showed that the expressions of CD44, DENND2B, MIB2 and RPL22L1 mRNAs were significantly upregulated in HSC4/CDDP cells (Fig. 4C),

Table 2
Primers used for the qRT-PCR assay.

Gene name		Sequence
ACER3	F	TGGACTGGTGCGAGGAGAACTAC
	R	GACCGTCTCTAACACTCTGAACTGC
ANAPC16	F	GGCTGCTTCATCATCATCCTCCTC
	R	GGGCAAGGTCTGAGACACTGAAAC
CD44	F	GAGCAGCACTTCAGGAGGTTACATC
	R	TCGGTGATCCAGGGACTGTCTTC
CNTNAP3	F	GGTTCAGGGAGTTTCGTCCTCTTTC
	R	TGCTGTGACATTCCTTGGTGACTG
DENND2B	F	GACAGCGACTCCGACGATGAATG
	R	GCCCTCTCTCCCTTCTCACTCTG
FAM111A	F	GGTCACGGAAGCACTCAGTCAATG
	R	TAGTTGTGGCTCTTGGGTCTCCTC
FANCI	F	CTATGTTTGCCAACCAGCTTGATGC
	R	ACCTGACTGACACTGAGAGACTGAC
GSN	F	TTGACTTCTGCTAAGCGGTACATCG
	R	CAAGGAACCAGCCCACAAAGGAG
LTBP4	F	GCGTGTGAAGAGGATGTGGATGAG
	R	GAAAGGAGCCTGCCGTGTTGTC
MIA2	F	CCTGACTGCCGATACCTGAACTTC
	R	TTCCTGCCCACAAATCTTCCCTTTC
MIB2	F	GACACCAAGAACCAAGGCAGGAC
	R	TTGTAGCAGCAGCCGTATCAACTC
PEX1	F	GTGGCTTTCTCAGAGGCAGTGTG
	R	CAGCAGGCAGTCCAGCAATGAG
RPL13A	F	GCCCGCCTCCTTACGACAAAAG
	R	CGGCAGAAAGACGACCAAGATGAC
RPL22L1	F	GCAGAAAGACAGGAAGCCCAAGAG
	R	CCCGAGATTTCCAGTTTTGCCATTG
SAMD9L	F	TTATTTCTTGGCCTGCCTCCTGTTC
	R	AAGTGTGCTTGCCTGCTTGGAC
SYTL1	F	GAGGCTGCTGTGAAAGAGAAGGAAG
	R	CAGAAGGCGATGGGAAATCAGGTC
TAZ	F	CATCACCATATCCAACCACCAGTCC
	R	CCATCTCATTCGCTTCAGGTTCCAG
TLK2	F	ATGGCATGGAGCTAACATCACAAGG
	R	CACCCACCGACCACACATCAAC
GAPDH	F	GGGAGCCAAAAGGGTCAT
	R	GAGTCCTTCCACGATACCAA

which were consistent with the sequencing data. However, the other 13 mRNAs showed no significant difference. These results made us focus on the significant gene CD44 with AS events in chemoresistance of OSCC.

GSEA analyzed the important role of CD44 in OSCC chemoresistance

We used GSEA analysis to predict and explore CD44 function in HNSCC. TCGA HNSCC data were divided into high and low groups according to CD44 expression and were analyzed with GMT file C2 KEGG and GO gene set profiles. All the enrichment results ($p < 0.05$ and FDR < 0.25) were shown in supplemental data Table S1. Many gene sets concerning cell adhesion regulation were enriched in the CD44 high expression HNSCC, such as focal adhesion pathway, adherens junction pathway, ECM-receptor interaction pathway, RHO protein signal transduction and regulation of actin cytoskeleton pathway. These were the key pathological pathways to predict the mechanism of OSCC occurrence and recurrence. Moreover, the upregulation of CD44 was significantly correlated with WNT signaling pathway, epidermal growth factor receptor signaling pathway, positive regulation of I-kappa B kinase NF kappa B cascade and ErbB signaling pathway (Fig. 5). Research showed that ErbB signal could regulate OSCC progression by mediating PI3K/Akt, which was consistent with our previous results in Fig. 2. Therefore, we speculated that CD44 might participate in the progression of OSCC.

CD44 associated with OSCC immune infiltration

The expression profiles of CD44 in human various cancers were analyzed using TCGA database combined with TIMER. The result showed that CD44 was upregulated in many solid cancers, including HNSCC (Fig. 6A). As immune cell infiltration provides valuable insights for the overall tumor microenvironment and better prognosis [14], we evaluated the relationship between CD44 and immune infiltration to reveal the pivotal role of CD44 in OSCC progression. TCGA-HNSCC data were firstly grouped into high and low groups by the median value of CD44 expression. Then, we employed the CIBERSORT algorithm to compare the 22 subpopulations of different immune cells in CD44-high or -low expression groups. Our findings demonstrated that CD44 expression was mainly relevant to the immune infiltration of T cells and dendritic cells (DCs) activation (Fig. 6B). Moreover, TIMER was used to evaluate the correlations of CD44 expression with tumor purity and immune cells infiltrating levels. The results showed that the CD44 expression had a close correlation with tumor purity and immune infiltration levels of HNSCC, including DCs (r =0.142, p = 1.78e-03), $CD8^+$ T cells (r = -0.144, p = 1.70e-03) and $CD4^+$ T cells (r = 0.21, p = 3.59e-06) (Fig. 6C). Various markers of immune cells from relevant research were selected to further analyzed in TIMER database (Table 3). The results showed that CD44 was positively correlated with majority gene markers of DCs, which was accordant with Fig. 6. These findings suggested that CD44 play important roles in HNSCC immune infiltration.

CD44 might mediate cisplatin resistance by activating DCs tumor immune response

As the initial antigen-presenting cells connecting innate immunity and adaptive immunity, DCs can induce tumor immune tolerance and promote tumor drug resistance [15]. In Fig. 6B and 6C, bio-informatics analysis predicted that more activated DCs infiltrated in high-CD44 expression group relative to low-CD44 expression group. In order to further investigate the relationship among CD44, DCs infiltration and chemoresistance, we first detected the expression of CD44 in CDDP resistant cell lines. The results showed that CD44 protein was significantly upregulated in drug-resistant cell lines, indicating that CD44 participated in the CDDP resistance of OSCC (Fig. 7A), which was consistent with previous mRNA expression (Fig. 4C). Then, we transfected CD44 overexpression plasmid into Cal27/HSC4 CDDP cell lines for gain-of-function study (Fig. 7B). The results showed that CD44 overexpression could significantly increase the IC_{50} value of CDDP resistant cells (Fig. 7C). Together with the bioinformatics prediction results, we further constructed a co-culture model using Cal27/HSC4 CDDP and DCs to explore the immune response induced by CD44 associated cisplatin resistance increasement. Compared with control group, the expression levels of DCs surface antigens were significantly increased in the CD44 overexpression co-culture model (Fig. 7D). These results showed that the high expression of CD44 could promote the maturation and activation of DCs in both drug-resistant and non-drug resistant cells, and further increase the drug resistance of CDDP resistant cells. However, CD44 overexpression led to a lower rate of activated DCs in drug-resistant cells compared with non-drug resistant cells (Fig. 7E). This made us speculate that CD44 may form different variants through AS, and then reduce the ability of DC cells to activate tumor immunity through different signaling pathways, thereby affecting the cisplatin resistance of OSCC.

Discussion

Most precursor mRNA only produce one mature mRNA after transcription and translate it into one polypeptide chain. However, some precursor mRNAs can be sheared or (and) spliced into several mRNAs with different structures and this process is called AS [16–18]. AS has been reported to be involved in a variety of physiological processes and contributes to the development of various cancers and drug resistance [19–23]. At present, survival related AS events have been identified through comprehensive analysis of TCGA OSCC data. A novel prognostic

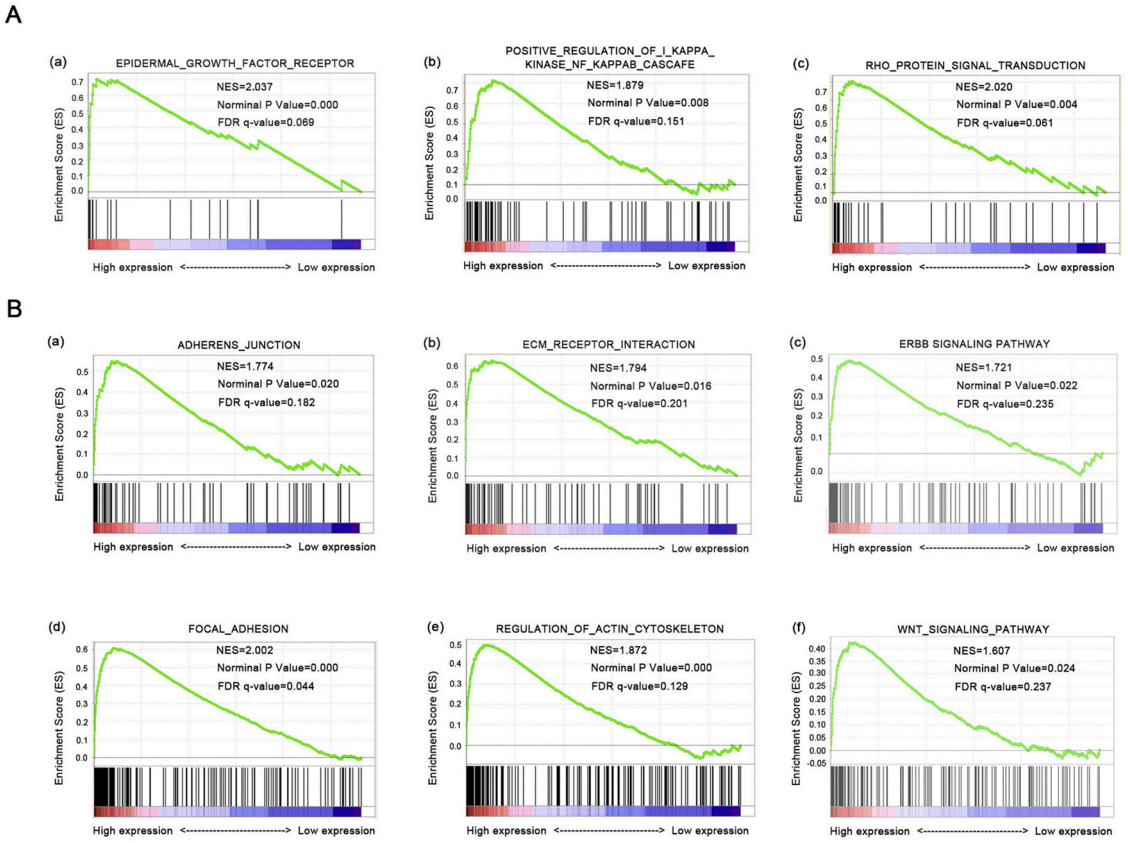

Fig. 5. CD44 promoted the progression of OSCC analyzed by GSEA. Gene set enrichment analysis was performed using the TCGA gene expression profiles of HNSCC. (A) Gene sets were enriched in CD44 high expression HNSCC according to 'c5 all v7.0' GO gene set profile. (B) Gene sets were enriched in CD44 high expression HNSCC according to 'c2.cp.kegg. v7.2' KEGG gene set profile.

AS model has been developed based on the sensitivity of 138 chemotherapeutic drugs in Genomics of Drug Sensitivity in Cancer (GDSC) [24,25]. However, the AS model of cisplatin resistance in OSCC has not been reported yet. In this study, we screened differentially expressed mRNA in cisplatin resistant OSCC cells and established a novel cisplatin resistant AS model. In this model, we found that SE (61.9%) was the most common AS event, which might play a major role in the chemoresistance of OSCC. Meanwhile, a total of 18 genes including CD44 participated in the resistance of OSCC to cisplatin, and these genes were differentially expressed with AS events. Therefore, it is essential to determine the function of AS alterations for understanding the chemoresistance mechanism in OSCC. Moreover, AS may be considered as a therapeutic target to provide new insights for relieving chemotherapy resistance.

CD44 is a hyaluronan binding cell surface adhesion molecule that influences tumor development, tumor metastasis, the formation of tumor microenvironment as well as the expression of chemotherapy resistance phenotype [26,27]. Previous studies have revealed that CD44 overexpression weakened the cytotoxicity of chemotherapy on various cancers, which led to poor prognosis of patients [26]. In this study, we found that CD44 occurring SE event led to the enhancement of cisplatin chemoresistance in OSCC, which was consistent with the study of Kashyap et al. [28]. Furthermore, targeting the activity of AS variants might be useful to activate or improve NK cell surveillance on various cancers including OSCC, while changes in the immune microenvironment could predict patient's response to chemotherapy [22]. Traditionally, DCs are considered to be the most effective initial antigen presenting cells, which can stimulate T cells and initiate anti-tumor immunity [29,30]. However, more studies have found that DCs activated by inflammatory factors could be transformed into DCs with immune regulation functions, leading to tumor immune tolerance and chemotherapy resistance [15,31]. Due to the cell maturity and microenvironment, there may be no contradiction between the anti-tumor immune initiation of DCs and the induction of tumor drug resistance. Our findings indicated that CD44 overexpression could promote the maturation and activation of DCs, no matter in co-cultured CDDP-resistant or non CDDP-resistant OSCC cells, which was consistent with bioinformatics prediction. Targeting CD44 activity may lay a foundation for studying the immune mechanism of cisplatin resistance in OSCC.

There are many variant isoforms of CD44, which are produced by alternative splicing of different combinations among 10 exons (v1–10). Different subtypes with various properties may have different tissue-specific effects, which contribute to diverse influence on cancer progression or drug resistance [27,28,32–35]. For example, the expression of CD44v9 might be used as a new indicator to identify the CDDP resistant population in patients with surgically treated urothelial carcinoma [32]. CD44v8–10 induces ROS defenses by promoting xCT function that regulates GSH synthesis, which contributes to chemotherapy resistance [32]. CD44v4 expression is more closely related to the activation of ERK1/2 and the aggravation of cisplatin resistance, while the expression of CD44v6 is mainly related to PI3K/Akt/GSK3β activation and the occurrence of tumor invasion or migration [28,35]. Combined with the current research on the drug resistance function and immune microenvironment regulation of AS, we speculate that CD44 may regulate different signaling pathways through different variants, thereby reducing the ability of DCs to activate tumor immunity and enhancing the cisplatin resistance of OSCC. We will confirm this in the subsequent studies.

In summary, our findings established the AS model of OSCC cisplatin resistant cell line and identified that CD44 occurring SE event could activate DC mediated tumor immune response and enhance the cisplatin resistance of OSCC. Targeting CD44 activity may not only provide a new

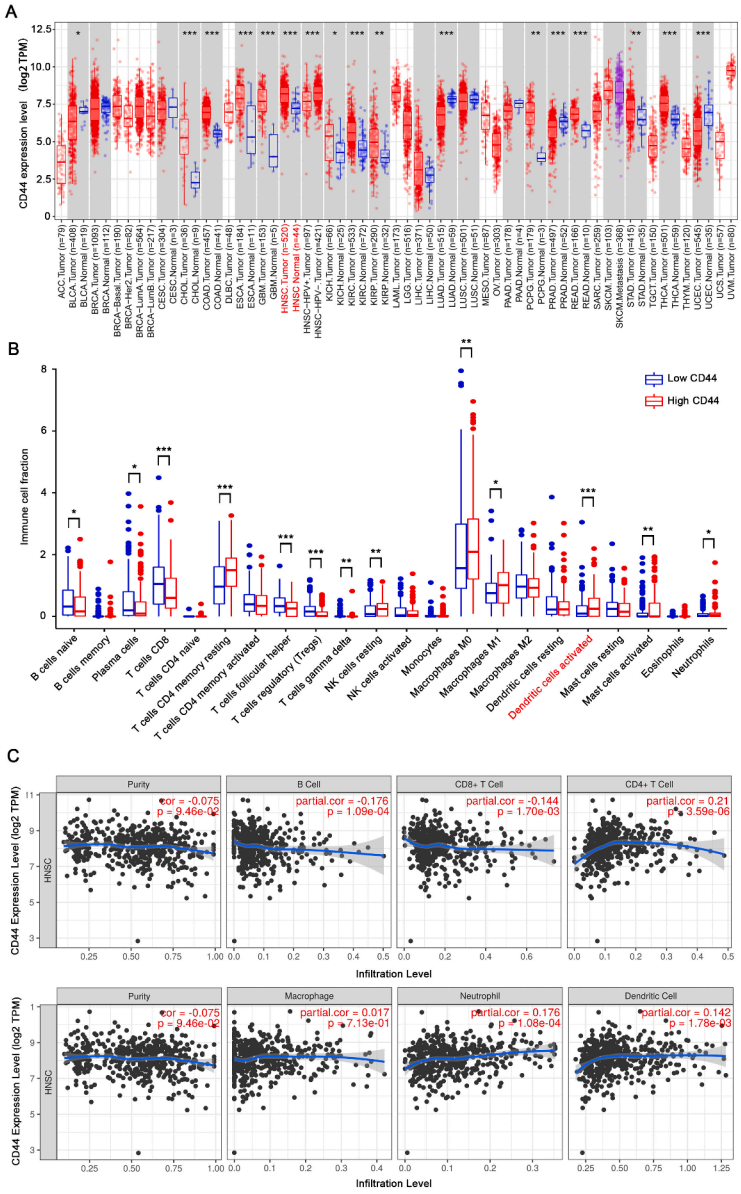

Fig. 6. CD44 may play an important role in immune infiltration of HNSCC. (A) CD44 expression profiles were analyzed through TIMER online tool from TCGA database. (B) Tumor infiltrated lymphocytes distributions were analyzed by CIBERSORT algorithm with R package according to CD44 expression. (C) Immune infiltration correlation with CD44 expression was analyzed by TIMER online analyses. *$P < 0.05$, **$P < 0.01$, ***$P < 0.001$, Student's *t*-test.

Table 3
Correlation analysis between CD44 and related genes and markers of immune cells in TIMER.

Description	Gene markers	HNSC (Total)				HNSC (HPV-pos)				HNSC (HPV-neg)			
		none cor	P	purity cor	P	none cor	P	purity cor	P	none cor	P	purity cor	P
CD8+ T cell	CD8A	-0.085	0.051	-0.061	0.176	-0.237	0.019	-0.210	0.047	0.026	0.589	0.036	0.466
	CD8B	-0.161	**	-0.143	*	-0.372	**	-0.354	**	-0.034	0.480	-0.032	0.529
	PTPRC	0.126	*	0.145	*	0.022	0.831	0.083	0.439	0.230	***	0.227	***
T cell (general)	CD3D	-0.160	**	-0.137	*	-0.384	***	-0.364	**	-0.039	0.429	-0.031	0.535
	CD3E	-0.076	0.085	-0.052	0.251	-0.269	*	-0.238	0.024	0.050	0.308	0.056	0.262
	CD2	-0.102	0.019	-0.082	0.071	-0.286	*	-0.264	0.012	0.023	0.641	0.026	0.597
B cell	CD19	-0.189	***	-0.169	**	-0.398	***	-0.358	**	-0.060	0.218	-0.058	0.250
	CD79A	-0.143	*	-0.122	*	-0.350	**	-0.308	*	-0.012	0.813	-0.009	0.857
	CD27	-0.143	*	-0.121	*	-0.343	**	-0.313	*	-0.015	0.752	-0.010	0.846
	CD20 (KRT20)	-0.080	0.068	-0.071	0.115	-0.088	0.388	-0.056	0.603	-0.084	0.086	-0.085	0.089
Monocyte	CD14	0.079	0.071	0.081	0.072	0.067	0.510	0.056	0.601	0.101	0.038	0.100	0.045
	CD115 (CSF1R)	0.141	*	0.153	**	0.065	0.524	0.084	0.432	0.199	***	0.199	***
TAM	CCL2	0.122	*	0.132	*	0.168	0.098	0.209	0.048	0.123	0.012	0.120	0.017
	CD68	0.271	***	0.279	***	0.377	**	0.375	**	0.270	***	0.279	***
	IL10	0.214	***	0.221	***	0.144	0.158	0.159	0.135	0.262	***	0.261	***
M1 Macrophage	INOS (NOS2)	-0.106	0.015	-0.096	0.033	-0.302	*	-0.291	*	0.040	0.410	0.033	0.507
	CD80	0.198	***	0.210	***	0.065	0.526	0.093	0.384	0.271	***	0.266	***
	IRF5	-0.034	0.444	-0.022	0.629	0.017	0.871	-0.003	0.981	0.021	0.661	0.032	0.516
	IL6	0.266	***	0.272	***	0.393	***	0.433	***	0.211	***	0.209	***
	CD64 (FCGR1A)	0.034	0.444	0.030	0.510	-0.029	0.779	-0.066	0.535	0.091	0.063	0.090	0.073
M2 Macrophage	CD163	0.208	***	0.197	***	0.281	*	0.258	0.014	0.213	***	0.208	***
	MRC1	0.317	***	0.303	***	0.325	*	0.302	*	0.295	***	0.292	***
	VSIG4	0.118	*	0.110	0.015	0.192	0.059	0.150	0.157	0.108	0.027	0.112	0.025
	MS4A4A	0.120	*	0.117	*	0.136	0.181	0.107	0.317	0.152	*	0.149	*
Neutrophils	CD66b (CEACAM8)	-0.141	*	-0.113	0.012	-0.106	0.297	-0.062	0.559	-0.075	0.122	-0.062	0.218
	CD11b (ITGAM)	0.027	0.544	0.037	0.407	-0.128	0.208	-0.112	0.293	0.124	0.011	0.121	0.016
	CD16 (FUT4)	0.286	***	0.293	***	-0.062	0.543	-0.035	0.740	0.413	***	0.405	***
Natural killer cell	KIR2DL1	0.013	0.768	0.028	0.542	0.002	0.981	-0.031	0.770	0.072	0.141	0.092	0.066
	KIR2DL3	-0.083	0.057	-0.069	0.126	-0.213	0.036	-0.223	0.034	0.016	0.737	0.030	0.554
	KIR3DL1	-0.095	0.031	-0.081	0.074	-0.335	**	-0.329	*	0.049	0.313	0.059	0.238
	KIR3DL2	-0.060	0.168	-0.054	0.233	-0.092	0.370	-0.093	0.384	0.022	0.650	0.023	0.650
	CD56 (NCAM1)	0.213	***	0.236	***	0.136	0.180	0.174	0.100	0.198	***	0.213	***
	CD335 (NCR1)	0.087	0.047	0.112	0.013	0.073	0.474	0.109	0.306	0.187	**	0.193	**
Dendritic cell	BDCA-1 (CD1C)	-0.003	0.950	0.020	0.658	-0.145	0.156	-0.119	0.265	0.097	0.046	0.106	0.033
	BDCA-3 (THBD)	0.163	**	0.153	**	0.283	*	0.273	*	0.121	0.013	0.119	0.017
	BDCA-4 (NRP1)	0.448	***	0.445	***	0.601	***	0.606	***	0.405	***	0.404	***
	CD123 (IL3RA)	-0.081	0.064	-0.059	0.192	-0.324	*	-0.311	*	0.016	0.750	0.024	0.630
	CD11c (ITGAX)	0.093	0.035	0.102	0.023	0.008	0.940	-0.005	0.964	0.149	*	0.156	*
Th1	T-bet (TBX21)	-0.092	0.036	-0.066	0.142	-0.255	0.011	-0.230	0.029	0.017	0.723	0.030	0.550
	STAT4	0.100	0.023	0.109	0.015	-0.105	0.304	-0.072	0.498	0.201	***	0.192	**
	STAT1	0.317	***	0.320	***	0.300	*	0.308	*	0.336	***	0.332	***
Th2	GATA3	0.073	0.097	0.073	0.105	0.002	0.985	0.042	0.697	0.109	0.026	0.093	0.064
	STAT6	0.285	***	0.288	***	0.210	0.038	0.209	0.048	0.354	***	0.350	***
	IL13	-0.052	0.234	-0.057	0.210	-0.064	0.532	-0.084	0.433	-0.013	0.789	-0.022	0.665
Tfh	BCL6	0.148	**	0.153	**	0.222	0.028	0.245	0.020	0.189	***	0.187	**
	IL21	0.020	0.642	0.026	0.562	-0.083	0.415	-0.037	0.731	0.109	0.025	0.088	0.079
Th17	STAT3	0.257	***	0.275	***	0.205	0.043	0.232	0.028	0.358	***	0.357	***
	IL17A	-0.023	0.594	-0.011	0.812	-0.064	0.530	-0.017	0.871	0.049	0.313	0.045	0.366
Treg	FOXP3	0.131	*	0.152	**	0.010	0.924	0.063	0.558	0.248	***	0.247	***
	ISG20	-0.063	0.153	-0.049	0.278	-0.207	0.040	-0.168	0.112	-0.019	0.701	-0.016	0.748
	CCR8	0.255	***	0.275	***	0.249	0.013	0.314	*	0.326	***	0.321	***
	STAT5B	0.222	***	0.238	***	0.294	*	0.350	**	0.250	***	0.253	***
T cell exhaustion	PD-1 (PDCD1)	-0.091	0.037	-0.070	0.123	-0.288	*	-0.260	0.013	0.029	0.558	0.034	0.503
	CTLA4	0.007	0.873	0.023	0.610	-0.209	0.039	-0.184	0.083	0.125	0.010	0.122	0.014
	LAG3	-0.068	0.119	-0.050	0.265	-0.228	0.024	-0.222	0.036	0.022	0.659	0.030	0.554
	TIM-3 (HAVCR2)	0.089	0.042	0.103	0.023	-0.018	0.859	-0.020	0.852	0.174	**	0.179	**
	GZMB	-0.077	0.079	-0.055	0.222	-0.229	0.023	-0.215	0.042	0.016	0.748	0.029	0.562

HNSCC, head and neck squamous cell carcinoma; HPV-pos, HPV positive; HPV-neg, HPV negative; None, correlation without adjustment; Purity, correlation adjusted by purity; TAM, tumor-associated macrophage; Th, T helper cell; Tfh, follicular helper T cell; Treg, regulatory T cell; Cor, R value of Spearman's correlation.
* $P<0.01$;
** $P<0.001$;
*** $P<0.0001$.

target for the treatment of OSCC, but also provide new insights for the study of cisplatin resistance.

Consent for publication

Not applicable.

Availability of data and material

The original contributions presented in the study are included in the article, further inquiries can be directed to the corresponding author on reasonable request.

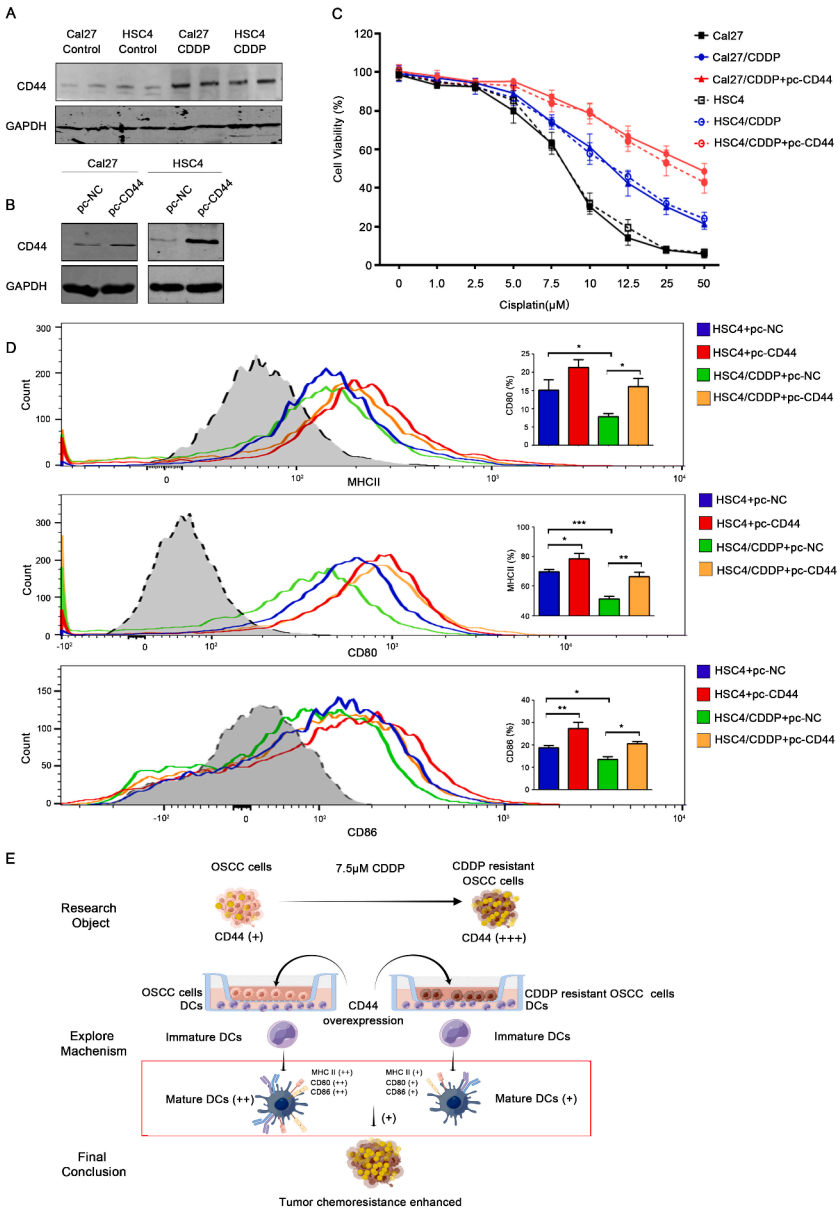

Fig. 7. CD44 promoted OSCC immune response and drug resistance. (A) CD44 was up-regulated in both Cal27/CDDP and HSC4/CDDP cells. Cal27 and HSC4 cells were used as controls. (B) CD44 was efficiently overexpressed through plasmid transfection for 48h. Cal27 and HSC4 cells were used as controls. (C) CCK8 assays were used to detect cell viability and IC_{50} value in Cal27/CDDP and HSC4/CDDP cells. Cal27 and HSC4 cells were used as controls. (D) Flow cytometry were used to detect CD80, CD86 and MHCII positive cell proportion in HSC4, HSC4/CDDP, CD44 overexpressed HSC4, and CD44 overexpressed HSC4/CDDP cells. All experiments were performed at least 3 times, data were shown as mean ± SD. $^{*}P < 0.05$, $^{**}P < 0.01$, $^{***}P < 0.001$ vs. control, Student's *t*-test. (E) Brief portrait was drawn and legally downloaded from Figdraw online tool to illustrate the regulation role of CD44 on OSCC chemoresistance through evoking DCs mediated immune response.

Funding

This study was funded by the National Nature Science Foundation of China (Grant number 81972535) and the Nature Science Foundation of Liaoning Province, China (Grant number 2021-MS-169).

Authors' contributions

YG, XQ, LZ and RS carried out the expression and biological behavior studies and performed the statistical analysis. **YG and XQ** designed and performed the bioinformatics and co-culture associated experiments. **YG and CS** conceived of the study and drafted the manuscript. All authors read and approved the final manuscript.

Fig. S1. Establishment of cisplatin resistant OSCC cells. (A-B) CCK8 assays were conducted in Cal27/CDDP and HSC4/CDDP cells. (C-D) Representative images of apoptosis in Cal27/CDDP and HSC4/CDDP cells treated with CDDP for 48h. Cal27 and HSC4 cells were used as controls. All experiments were performed at least 3 times; data were shown as mean ± SD. $^{*}P < 0.05$, $^{**}P < 0.01$, $^{***}P < 0.001$ vs. control, Student's *t*-test.

Declaration of Competing Interest

The authors declare that they have no known competing financial interests or personal relationships that could have appeared to influence the work reported in this paper.

Acknowledgements

Not applicable.

Supplementary materials

Supplementary material associated with this article can be found, in the online version, at doi:10.1016/j.tranon.2023.101644.

References

[1] D.E. Johnson, B. Burtness, C.R. Leemans, V.W.Y. Lui, J.E. Bauman, J.R. Grandis, Head and neck squamous cell carcinoma, Nat. Rev. Dis. Primers 6 (1) (2020) 92.

[2] A. Chamoli, A.S. Gosavi, U.P. Shirwadkar, K.V. Wangdale, S.K. Behera, N. K. Kurrey, K. Kalia, A. Mandoli, Overview of oral cavity squamous cell carcinoma: risk factors, mechanisms, and diagnostics, Oral Oncol. 121 (2021), 105451.
[3] X. Qiao, L. Zhu, R. Song, C. Shang, Y. Guo, METTL3/14 and IL-17 signaling contribute to CEBPA-DT enhanced oral cancer cisplatin resistance, Oral Dis. (2021), https://doi.org/10.1111/odi.14083.
[4] C.C. Hung, C.Y. Chien, P.Y. Chu, Y.J. Wu, C.S. Lin, C.J. Huang, L.P. Chan, Y. Y. Wang, S.F. Yuan, T.C. Hour, et al., Differential resistance to platinum-based drugs and 5-fluorouracil in p22phox-overexpressing oral squamous cell carcinoma: Implications of alternative treatment strategies, Head Neck 39 (8) (2017) 1621–1630.
[5] X. Liu, Y. Zhang, W. Lu, Y. Han, J. Yang, W. Jiang, X. You, Y. Luo, S. Wen, Y. Hu, et al., Mitochondrial TXNRD3 confers drug resistance via redox-mediated mechanism and is a potential therapeutic target *in vivo*, Redox Biol. 36 (2020), 101652.
[6] A. Kumar, I. Coleman, C. Morrissey, X. Zhang, L.D. True, R. Gulati, R. Etzioni, H. Bolouri, B. Montgomery, T. White, et al., Substantial interindividual and limited intraindividual genomic diversity among tumors from men with metastatic prostate cancer, Nat. Med. 22 (4) (2016) 369–378.
[7] C. Kim, R. Gao, E. Sei, R. Brandt, J. Hartman, T. Hatschek, N. Crosetto, T. Foukakis, N.E. Navin, Chemoresistance evolution in triple-negative breast cancer delineated by single-cell sequencing, Cell 173 (4) (2018) 879–893, e813.
[8] Y. Cheng, S. Li, L. Gao, K. Zhi, W. Ren, The molecular basis and therapeutic aspects of cisplatin resistance in oral squamous cell carcinoma, Front. Oncol. 11 (2021), 761379.
[9] U. Mehraj, A.H. Dar, N.A. Wani, M.A. Mir, Tumor microenvironment promotes breast cancer chemoresistance, Cancer Chemother. Pharmacol. 87 (2) (2021) 147–158.
[10] S. Böhm, A. Montfort, O.M. Pearce, J. Topping, P. Chakravarty, G.L. Everitt, A. Clear, J.R. McDermott, D. Ennis, T. Dowe, et al., Neoadjuvant chemotherapy modulates the immune microenvironment in metastases of tubo-ovarian high-grade serous carcinoma, Clin. Cancer Res. 22 (12) (2016) 3025–3036.
[11] D. Roy Burman, S. Das, C. Das, R. Bhattacharya, Alternative splicing modulates cancer aggressiveness: role in EMT/metastasis and chemoresistance, Mol. Biol. Rep. 48 (1) (2021) 897–914.
[12] S. Shen, J.W. Park, Z.X. Lu, L. Lin, M.D. Henry, Y.N. Wu, Q. Zhou, Y. Xing, rMATS: robust and flexible detection of differential alternative splicing from replicate RNA-Seq data, Proc. Natl. Acad. Sci. USA 111 (51) (2014) E5593–E5601.
[13] G. Dixit, Y. Zheng, B. Parker, J. Wen, Identification of alternative splicing and polyadenylation in RNA-seq data, J. Vis. Exp. (172) (2021), https://doi.org/10.3791/62636.
[14] Z.X. Li, Z.Q. Zheng, Z.H. Wei, L.L. Zhang, F. Li, L. Lin, R.Q. Liu, X.D. Huang, J. W. Lv, F.P. Chen, et al., Comprehensive characterization of the alternative splicing landscape in head and neck squamous cell carcinoma reveals novel events associated with tumorigenesis and the immune microenvironment, Theranostics 9 (25) (2019) 7648–7665.
[15] S.K. Wculek, F.J. Cueto, A.M. Mujal, I. Melero, M.F. Krummel, D. Sancho, Dendritic cells in cancer immunology and immunotherapy, Nat. Rev. Immunol. 20 (1) (2020) 7–24.
[16] S. Oltean, D.O. Bates, Hallmarks of alternative splicing in cancer, Oncogene 33 (46) (2014) 5311–5318.
[17] E. El Marabti, I. Younis, The cancer spliceome: reprograming of alternative splicing in cancer, Front. Mol. Biosci. 5 (2018) 80.
[18] E.T. Wang, R. Sandberg, S. Luo, I. Khrebtukova, L. Zhang, C. Mayr, S.F. Kingsmore, G.P. Schroth, C.B. Burge, Alternative isoform regulation in human tissue transcriptomes, Nature 456 (7221) (2008) 470–476.
[19] B.D. Wang, N.H. Lee, Aberrant RNA splicing in cancer and drug resistance, Cancers 10 (11) (2018) 458, https://doi.org/10.3390/cancers10110458.
[20] L. Escobar-Hoyos, K. Knorr, O. Abdel-Wahab, Aberrant RNA splicing in cancer, Annu. Rev. Cancer Biol. 3 (1) (2019) 167–185.
[21] Y. Sun, L. Yan, J. Guo, J. Shao, R. Jia, Downregulation of SRSF3 by antisense oligonucleotides sensitizes oral squamous cell carcinoma and breast cancer cells to paclitaxel treatment, Cancer Chemother. Pharmacol. 84 (5) (2019) 1133–1143.
[22] W. Gao, S. Xu, M. Zhang, S. Liu, S.P. Siu, H. Peng, J.C. Ng, G.S. Tsao, A.W. Chan, V. L. Chow, et al., NADPH oxidase 5α promotes the formation of CD271 tumor-initiating cells in oral cancer, Am. J. Cancer Res. 10 (6) (2020) 1710–1727.
[23] X. Wang, J. Guo, X. Che, R. Jia, PCBP1 inhibits the expression of oncogenic STAT3 isoform by targeting alternative splicing of STAT3 exon 23, Int. J. Biol. Sci. 15 (6) (2019) 1177–1186.
[24] S. Zhang, X. Wu, P. Diao, C. Wang, D. Wang, S. Li, Y. Wang, J. Cheng, Identification of a prognostic alternative splicing signature in oral squamous cell carcinoma, J. Cell. Physiol. 235 (5) (2020) 4804–4813.
[25] R. Cao, J. Zhang, L. Jiang, Y. Wang, X. Ren, B. Cheng, J. Xia, Comprehensive analysis of prognostic alternative splicing signatures in oral squamous cell carcinoma, Front. Oncol. 10 (2020) 1740.
[26] Z. Yaghobi, A. Movassaghpour, M. Talebi, M. Abdoli Shadbad, K. Hajiasgharzadeh, S. Pourvahdani, B. Baradaran, The role of CD44 in cancer chemoresistance: a concise review, Eur. J. Pharmacol. 903 (2021), 174147.
[27] L. Prochazka, R. Tesarik, J. Turanek, Regulation of alternative splicing of CD44 in cancer, Cell. Signal. 26 (10) (2014) 2234–2239.
[28] T. Kashyap, K.K. Pramanik, N. Nath, P. Mishra, A.K. Singh, S. Nagini, A. Rana, R. Mishra, Crosstalk between Raf-MEK-ERK and PI3K-Akt-GSK3β signaling networks promotes chemoresistance, invasion/migration and stemness via expression of CD44 variants (v4 and v6) in oral cancer, Oral Oncol. 86 (2018) 234–243.
[29] D. Chauhan, A.V. Singh, M. Brahmandam, R. Carrasco, M. Bandi, T. Hideshima, G. Bianchi, K. Podar, Y.T. Tai, C. Mitsiades, et al., Functional interaction of plasmacytoid dendritic cells with multiple myeloma cells: a therapeutic target, Cancer Cell 16 (4) (2009) 309–323.
[30] A. Gardner, Á. de Mingo Pulido, B. Ruffell, Dendritic cells and their role in immunotherapy, Front. Immunol. 11 (2020) 924.
[31] D.A. Chistiakov, A.N. Orekhov, Y.V. Bobryshev, Dendritic cells in colorectal cancer and a potential for their use in therapeutic approaches, Curr. Pharm. Des. 22 (16) (2016) 2431–2438.
[32] M. Hagiwara, E. Kikuchi, N. Tanaka, T. Kosaka, S. Mikami, H. Saya, M. Oya, Variant isoforms of CD44 involves acquisition of chemoresistance to cisplatin and has potential as a novel indicator for identifying a cisplatin-resistant population in urothelial cancer, BMC Cancer 18 (1) (2018) 113.
[33] C.C. Warzecha, T.K. Sato, B. Nabet, J.B. Hogenesch, R.P. Carstens, ESRP1 and ESRP2 are epithelial cell-type-specific regulators of FGFR2 splicing, Mol. Cell 33 (5) (2009) 591–601.
[34] B.H. Li, S.B. Xu, F. Li, X.G. Zou, A. Saimaiti, D. Simayi, Y.H. Wang, Y. Zhang, J. Yuan, W.J. Zhang, Stat6 activity-related Th2 cytokine profile and tumor growth advantage of human colorectal cancer cells *in vitro* and *in vivo*, Cell. Signal. 24 (3) (2012) 718–725.
[35] M. Salmi, K. Grön-Virta, P. Sointu, R. Grenman, H. Kalimo, S. Jalkanen, Regulated expression of exon v6 containing isoforms of CD44 in man: downregulation during malignant transformation of tumors of squamocellular origin, J. Cell Biol. 122 (2) (1993) 431–442.